Received: 7 November 2016 | Revised: 17 April 2018 | Accepted: 22 September 2019

DOI: 10.1002/bio.3721

RESEARCH ARTICLE

WILEY LUMINESCENCE
The Journal of Biological and Chemical Luminescence

Synthesis and characterization of luminescent SiO_2@Eu(phen–Si) core–shell nanospheres

Wen-Xian Li[1] | Yu-Shan Zheng[2] | Hong-Bo Zhang[2] | Jin-Rong Bao[1] | Yi-Lian Li[1] | Yang-Yang Ma[1] | Li-Na Feng[1] | Shu-Yan Feng[1]

[1] College of Chemistry and Chemical Engineering, Inner Mongolia University, Hohhot, People's Republic of China

[2] Inner Mongolia Autonomous Region Food Inspection Testing Center, Hohhot, People's Republic of China

Correspondence
Wen-Xian Li, College of Chemistry and Chemical Engineering, Inner Mongolia University, Hohhot 010021, People's Republic of China.
Email: nmglwx@163.com

Funding information
Major projects of Natural Science Foundations of Inner Mongolia Science Foundation, Grant/Award Number: 2015ZD01; Natural Science Foundations of Inner Mongolia Science Foundation, Grant/Award Number: 2015MS0502

Abstract

Four core–shell structured nanometre luminescent composites with different kernel sizes and different shell layer thicknesses ($SiO_{2(500)}$@Eu (phen–Si)$_{(50)}$, $SiO_{2(500)}$@Eu (phen–Si)$_{(15)}$, $SiO_{2(250)}$@Eu (phen–Si)$_{(5)}$ and $SiO_{2(250)}$@Eu (phen–Si)$_{(10)}$) were made by changing synthesis conditions. Here, initial subscript numbers in parentheses refer to the particle size of the SiO_2 core, whereas the final subscript numbers in parentheses refer to shell layer thickness. In these composites, silica spheres of 500 nm or 250 nm were identified as the core. The shell layer was composited of silicon, 1,10-phenanthroline and europium perchlorate, abbreviated as Eu(phen–Si); the chemical formula of phen–Si was phen-N-(CONH $(CH_2)Si(OCH_2CH_3)_3)_2$. The composites were characterized by scanning electron microscopy (SEM), transmission electron microscopy (TEM), and infrared spectroscopy. The monodispersed spherical SiO_2 showed characteristics of a regular microstructure and a smooth surface, as well as the advantage of dispersity, shown by SEM. The Eu(phen–Si) complex was able to self-assemble into monodispersed SiO_2 spheres, as seen using TEM.

Fluorescence spectra indicated that the four composites had excellent luminescence properties. Furthermore, composites composed of a SiO_2 core and a 250 nm kernel size exhibited stronger fluorescence than 500 nm kernel-sized composites. Fluorescence properties were affected by shell thickness: the thicker the shell, the greater the fluorescence intensity. For the four composites, quantum yield values and fluorescence lifetime corresponded to fluorescence emission intensity data as quantum yield values and fluorescence lifetime were higher, and luminescence properties increased.

KEYWORDS

europium perchlorate complex shell, fluorescence, fluorescence life time, quantum yieldSiO_2 core

1 | INTRODUCTION

Core–shell nanometre composites are a new style of structural material that can be assembled stably. Chemical bonds or other types of affinity contribute to the form in which a nanometre material is covered with another nanometre material. Nanometre composites produce a higher standard of structural material. Difference between core–shell nanometre composites and single compounds are due to

Abbreviations used: IR, Infrared; SEM, Scanning electron microscopy; TEM, Transmission electron microscopy; TEOS, Tetraethyl orthosilicate; TEPIC, 3-(Triethoxysilyl)-propyl isocyanate

the novel attributes of the composite, as described previously.[1–6] Core–shell nanometre materials can be widely applied as functional fluorescent materials, magnetic materials, and in electronics, medicine, and biological applications.[7–12] Chemical and optical characteristics in nanometre particles can be enhanced by covering these with a layer of another material, by altering features of the coating layer such as structure, thickness, size, or by composition. Some studies have described lower toxicity, larger efficient Stokes' conversion, intense release bands, and photochemical decrease for nanometre particles. The structure of a SiO_2 core and a shell, to some extent, contributes to improvements in luminescent materials. Some studies have reported changes in the advantageous attributes of luminescence intensity, efficient fluorescence quantum yield, and fluorescence lifetime found with the nanometre core–shell structure. In addition, changes in these features were due to the coordinating influence of the multi-element complex, not just because of simplified coordinated behaviour. It is important to establish new approaches to improve the design of the core–shell structure. SiO_2 is considered one of the most important and extensive core materials and is used world-wide due to its unique features such as formation of spherical monodispersed particles, simple manipulation of particle size, low cost, and security, as well as lower toxicity compared with other core materials. Some studies have shown that when SiO_2 is used as a core material, extremely strong affinity is always found between Si–OH groups and exterior hydrogen bonds on the surface. In addition, a few studies have described that the materials that are joined by chemical bonds and electrostatic interactions are formed easily. Crucial advanced features such as the size and morphology of SiO_2 composites are manipulated easily, a vital study area for nanometre materials. Research into SiO_2 and its use as a core material has increased widely and significantly in recent years, incorporating rare earth inorganic materials as the coating layer, but very few rare earth organic complexes have been used and applied as coating layers.[13–27]

Two crucial technologies have been applied to prepare the core–shell material. One technology is direct deposition, however performance of the core–shell material was limited when using this technology, as the material was not stable to ultrasound. The other technology is silane coupling. Silane coupling agents are organic materials with two functions. Their formula is defined as $Y(CH_2)_nSiX_3$ when used in the preparation of hybrid materials[24–28], where Y is organic functional groups such as amino, carboxyl, or double nitrogen, and X is an alkoxy group. This chemical formula ensures that the Y group can be assembled easily with rare earth ions. Some research has indicated that the chemical bonds for Si–O–Si could be hydrolyzed, referring to the chemical reaction between the X group and hydroxyl groups in SiO_2. Therefore rare earth ions could be combined with SiO_2 using a silane coupling agent, a process defined as a 'molecular bridge', to produce an inorganic–organic hybrid material. Vibrations in the bonds have been found with this type of hybrid material. However, energy loss was markedly decreased and luminous efficiency of the rare earth ions was enhanced, as shown in the study by Yan Bing and Zhang Hong Jie.[28–33] The present study focused on the composition and synthesis of core–shell structural materials. The SiO_2 sphere was selected as the core, and a rare earth organic complex was chosen to be the shell, which were combined with a silane coupling agent. Core–shell materials incorporate chemical bonds between the SiO_2 core and the coating material.[34–37] By using the silane coupling method, the performance the material remained unaltered and chemical bonds were stable, in addition the material was difficult to manipulate. The rare earth organic complex was applied as a coating layer at nanometre scale thickness, therefore the amount of rare earth organic complex was able to be decreased, consequently decreasing the cost of materials. The rare earth complex was able to be compatibly repaired by the SiO_2 core and the improvement in luminous efficiency was significant when comparing hybrid materials. Conversely, the structure of the core–shell, which is almost equivalent in size to the SiO_2 core, including the cladding layer thickness, affected fluorescence performance.

In the current study, a chemical with formula phen-N-$(CONH(CH_2)Si(OCH_2CH_3)_3)_2$, abbreviated to phen–Si, was used as the silane coupling agent. The double nitrogen atoms of phen–Si groups are able to assemble easily with rare earth europium ions. Si–O–Si bonds undergo hydrolysis involving a chemical reaction between three ethoxy groups in phen–Si and hydroxyl groups found in SiO_2 core spheres. Consequently, rare earth Eu ions and the SiO_2 core can be combined by a 'molecular bridge' determined by phen–Si, and primarily used to boost the attributes of the compound material. Very few studies have focused on rare earth organic materials combined with a SiO_2 core and shell (to give SiO_2@RE(phen–Si)). The molecular bridge improved luminescence properties such as brightness and intensity. In addition, due to the reduced thickness of the shell, consumption, and cost of the rare earth was much less, making it favourable for use.

In the present study, four nanometre luminescent complexes with core–shell structures of different kernel sizes and shell layer thicknesses ($SiO_{2(500)}$@Eu(phen–Si)$_{(50)}$, $SiO_{2(500)}$@Eu(phen–Si)$_{(15)}$, $SiO_{2(250)}$@Eu(phen–Si)$_{(5)}$ and $SiO_{2(250)}$@Eu(phen–Si)$_{(20)}$)) were made by changing the synthesis conditions (that is using 500 nm or 250 nm silica spheres as the core, and the phen–Si–Eu(III) complex as the shell layer (abbreviated to Eu(phen–Si)). Preparation of the nanometre luminescence composites is described.

2 | MATERIALS AND METHODS

2.1 | Materials

Purity of chemicals used in the present study, such as Eu_2O_3, exceeded 99.99%. To make europium perchlorate (abbreviated to Eu (III) perchlorate) the relevant oxide from perchloric acid ($HClO_4$) (1 mol/L) was used. 1,10-Phenanthroline was used as the starting material without further purification. Tetraethoxysilane (TEOS, Aldrich), 5% Pd/C (Aldrich) and 3-(triethoxysilyl)-propyl isocyanate (96%, TEPIC, Aldrich) were applied as received. Hydrazine monohydrate, H_2O_2 (30%), hexane, concentrated H_2SO_4 and HNO_3 and other chemicals were of analytical analysis grade.

2.2 | Physical measurements

Infrared spectra (IR, v = 400–4000 cm^{-1}) were prepared according to the KBr pressed disc method using a spectrophotometer, assembled as a Nicolet NEXUS-670 FT-IR spectrometer. ^{1}HNMR spectra were prepared using DMSO-d_6 and a Bruker AC-500 nuclear magnetic resonance spectrophotometer. Emission spectra and fluorescence excitation were confirmed using a FLS920 fluorescence photometer with a 1-nm slit width. Fluorescence decay curves were determined using a FLS920 Combined Steady State and Lifetime spectrometer. Microstructure was confirmed using SEM and TEM on Hitachi S-4800 and FEI Tecnai F20 instruments, respectively.

2.3 | Synthesis of the ligand phen–Si

The synthesis of phen–Si is shown in Scheme 1. The phen–Si ligand was synthesized using published techniques[38] and was a white solid. The solid was purified through recrystallization from alcohol. Element values were: yield: 40%. mp: 46–48°C. Anal. calcd. for $C_{32}H_{51}N_5O_8Si_2$ (M = 689 g/mol): C, 56.23%; H, 7.31%; N, 10.21%, found: C, 55.73%; H, 7.43%; N, 10.16%. ^{1}HNMR: δ0.45 ppm (2H, –CH_2–), δ1.43 ppm (2H, –CH_2–), δ3.06 ppm (2H, –CH_2–), δ3.70 ppm (12H,–CH_2–), δ1.12 ppm (18H, –CH_3), δ7.8 ppm (2H, –NH–).

2.4 | Synthesis of the SiO_2@Eu(phen–Si) core–shell structure nanometre luminescent composites

2.4.1 | Synthesis of monodispersed spherical SiO_2

Cores were identified to be monodispersed spherical SiO_2 formed based on Stöber.[39] Information in Table 1 is focused on the moderate dosage of anhydrous ethanol, water, ammonia solution, and TEOS. SiO_2 microspheres of different sizes were formed; 250 nm and 500 nm values were found using the average diameter for SiO_2 and confirmed by SEM.

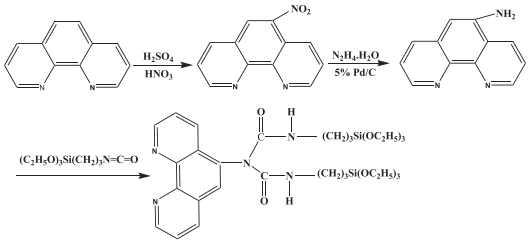

SCHEME 1 Synthesis of phen–Si

TABLE 1 Preparation conditions of monodisperse spherical SiO_2

Average diameter	CH_3CH_2OH (ml)	H_2O (ml)	TEOS (ml)	NH_3H_2O (ml)	Time (h)
250 nm	5	2	0.5	0.39	2
500 nm	5	2	0.5	0.65	2

2.4.2 | SiO_2 cores were grafted by phen–Si

For the grafting process, as described previously, chemical bonds in Si–O–Si can be hydrolyzed through three ethoxy groups in phen–Si and hydroxyl groups on the SiO_2 core surface. The SiO_2 core was coated by phen–Si through this interaction. Double nitrogen atoms in phen–Si can interact with rare earth ions. Different modification conditions were used for grafted composites such that different shell thickness were obtained. The details are as follows.

For phen–Si:SiO_2:ethanol volume = 0.1 g:0.1 g:10 ml, 0.1 g phen–Si was dissolved in 5 ml anhydrous alcohol; 0.1 g SiO_2 microspheres (500 nm or 250 nm) were dissolved in a mixture composed of anhydrous alcohol and distilled water, respectively. Both solutions (5 ml) were dispersed for about 10 min using ultrasound. The pH was adjusted using ammonia. Then, the phen–Si anhydrous alcohol solution was added dropwise to the activated SiO_2 microspheres solution. The mixture was stirred for 2 h at room temperature, and then separated by centrifugation at 5000 rpm. The resulting white precipitate was washed several times with water and anhydrous ethanol until the washing liquid was clear. Drying at 40°C was commenced. Two grafted SiO_2 cores of different shell layer thickness ($SiO_{2(500)}$@Eu (phen–Si)$_{(50)}$ and $SiO_{2(250)}$@Eu (phen–Si)$_{(10)}$) were then obtained.

For phen–Si:SiO_2:ethanol volume = 1 g:1 g:10 ml, using the previous method. Two grafted SiO_2 microspheres of different shell layer thickness ($SiO_{2(500)}$@Eu (phen–Si)$_{(15)}$ and $SiO_{2(250)}$@Eu (phen–Si)$_{(5)}$) were obtained.

2.4.3 | Self-assembly of the europium perchlorate organic core–shell structure nanometre luminescent composite (SiO_2@Eu(phen–Si))

Europium ions were self-assembled with the SiO_2 cores through a molecular bridge determined by phen–Si. Double nitrogen atoms of phen–Si groups on the grafted SiO_2 microspheres shell interact with Eu ions. Therefore, the SiO_2 core was coated with the Eu(III) perchlorate phen–Si complex through chemical bonds. Four kinds of modified SiO_2 microspheres were dissolved in 20 ml anhydrous ethanol, and dispersed using ultrasound for about 10 min. The molar ratio of Eu^{3+}:phen–Si was 1:2, a moderate dose of Eu perchlorate was dissolved in 5 ml anhydrous ethanol. The resulting solution was then added dropwise to the anhydrous ethanol solution of modified SiO_2 microspheres. The mixture was stirred for 30 min at room temperature, and then separated by centrifugation at 5000 rpm. The resulting white precipitate was washed several times with anhydrous ethanol and then dried. Four types of the white nanometre luminescent complex that formed the core–shell structure ($SiO_{2(500)}$@Eu(phen–Si)$_{(50)}$, $SiO_{2(500)}$@Eu(phen–Si)$_{(15)}$, $SiO_{2(250)}$@Eu(phen–Si)$_{(5)}$ and $SiO_{2(250)}$@Eu (phen–Si)$_{(10)}$) were obtained.

3 | RESULTS AND DISCUSSION

3.1 | SEM of monodisperse spherical SiO_2

SEM photographs showing features of the monodispersed spherical SiO_2 are shown in Figure 1 demonstrating the regular microstructure, smooth surface, and moderate dispersity. Here, a 250 nm and 500 nm average particle size of SiO_2 spheres.

3.2 | TEM of the SiO_2@Eu (phen–Si) core–shell structure nanometre luminescent composites

TEM photographs show the $SiO_{2(250)}$@Eu $(phen–Si)_{(5)}$ and $SiO_{2(250)}$@Eu $(phen–Si)_{(10)}$ nanometre luminescent structures (Figures 2 and 3). The size of the SiO_2 kernel was *c*. 250 nm. The SiO_2 core surface was clad with a thin layer of *c*. 5 nm or 10 nm, europium complexes and double nitrogen atoms in the phen–Si groups on the surface of the SiO_2 core were made using $Eu(ClO_4)_3$. This was further confirmed by infrared spectra. TEM photographs of the $SiO_{2(500)}$@Eu$(phen–Si)_{(15)}$ nanometre luminescent structures are shown in Figure 4. The size of the SiO_2 kernel was *c*. 500 nm. The surface of the SiO_2 core also was clad with a thin layer of *c*. 15 nm. The thin shell also was made up of europium complexes in which the double nitrogen atoms of phen–Si groups on the surface of the SiO_2 core coordinated with Eu $(ClO_4)_3$. This was further confirmed by infrared spectra. TEM photographs of the $SiO_{2(500)}$@Eu $(phen–Si)_{(50)}$ nanometre luminescent structure are shown in Figure 5. The interface of the coating layer of the Eu (phen–Si) complex and the SiO_2 core was clearly seen in the photographs. TEM photographs showed that the size of the SiO_2 kernel was *c*. 500 nm, and the surface of the SiO_2 core was clad in a shell layer. The thickness of the grey shell layer was *c*. 50 nm, and core–shell composition was clearly shown in the TEM photographs. EDX spectra (Figure 6) of composites of SiO_2 core and shell $SiO_{2(500)}$@Eu $(phen–Si)_{(50)}$ indicated the emission peaks of europium in the coating layer of the core–shell composite, demonstrating that the europium complex contained a coating layer. The SiO_2 cores were clad with the Eu(phen–Si)complex resulting in the synthesis of the SiO_2@Eu (phen–Si) core–shell structure.

3.3 | Formation of the core–shell structure nanometre luminescent composite

Synthesis of the composites from the SiO_2 core and shell is shown in Scheme 2. Chemical bonds in Si–O–Si were established via hydrolysis, by a chemical reaction between ethoxy groups in phen–Si and hydroxyl groups in SiO_2 core spheres. This process indicated that double nitrogen atoms in phen–Si groups on the grafted SiO_2 microspheres shell were able to interact with Eu(III) perchlorate. SiO_2 cores and Eu^{3+} ions were combined by a 'molecular bridge', determined from phen–Si. The rim of SiO_2 core was clad by the Eu(phen–Si) complex.

3.4 | Infrared spectra

The IR spectra of phen–Si, SiO_2, $SiO_{2(500)}$@Si-phen and $SiO_{2(500)}$@Eu $(phen–Si)_{(50)}$ can be seen in Figure S1(a–d). The IR spectra of the four nanometre luminescent composites formed by the core–shell structure are very similar. IR spectra indicated that the composition of the shell layer was the most significant factor that contributed to the composition of the Eu–phen–Si complex.

The phen–Si IR spectra presented here (Figure S1a), demonstrated vC=O group stretching at 1708 cm^{-1}. The vC=O stretching frequency

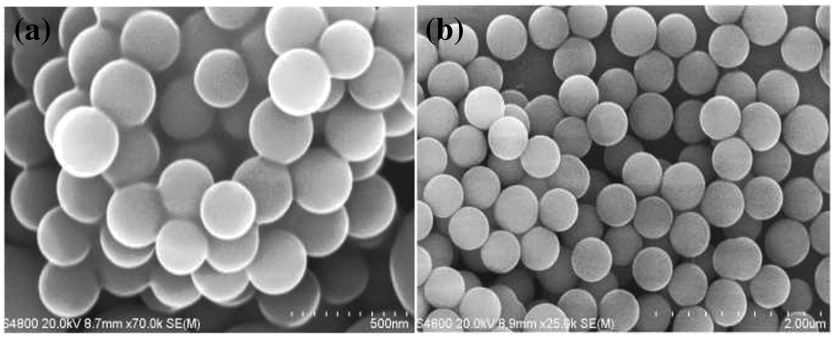

FIGURE 1 SEM photograph of (a) SiO_2 250 nm; (b) SiO_2 500 nm

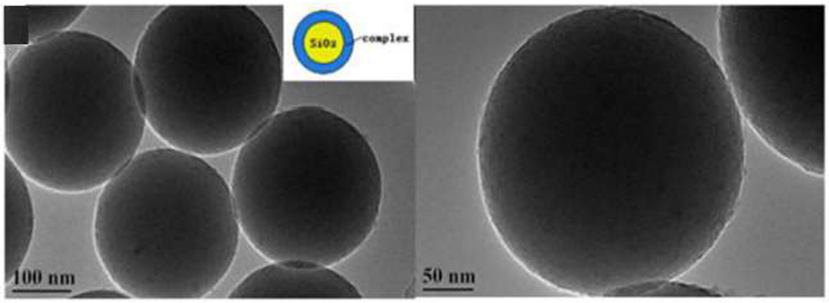

FIGURE 2 TEM photograph of $SiO_{2(250)}$@Eu $(phen–Si)_{(5)}$

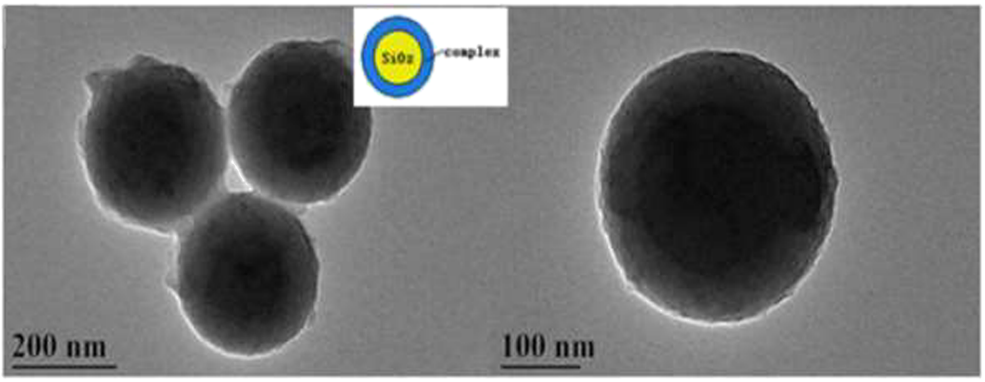

FIGURE 3 TEM photograph of $SiO_{2(250)}$@Eu(phen–Si)$_{(10)}$

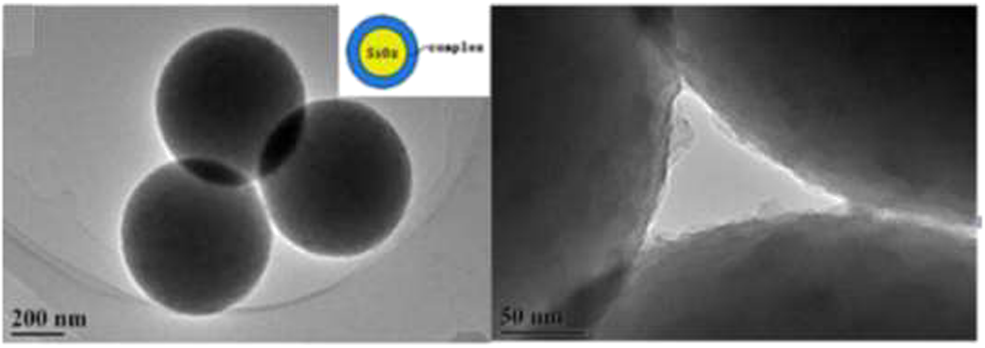

FIGURE 4 TEM photograph of $SiO_{2(500)}$@Eu(phen–Si)$_{(15)}$

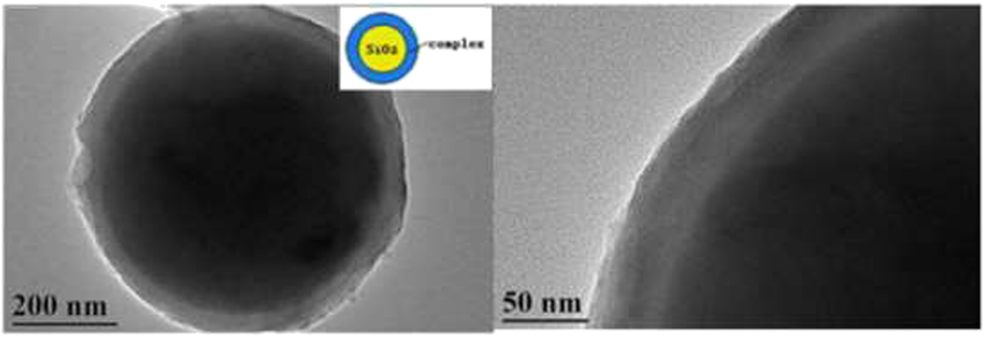

FIGURE 5 TEM photograph of $SiO_{2(500)}$@Eu(phen–Si)$_{(50)}$

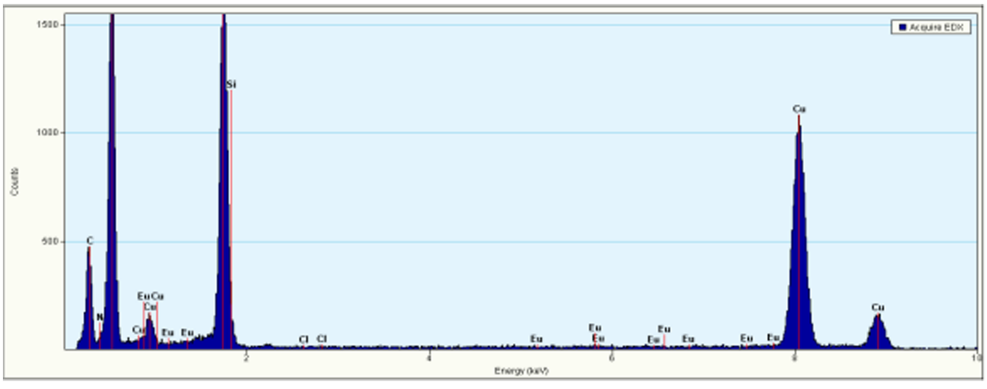

FIGURE 6 EDX spectrum of core–shell structure $SiO_{2(500)}$@Eu(phen–Si)$_{(50)}$

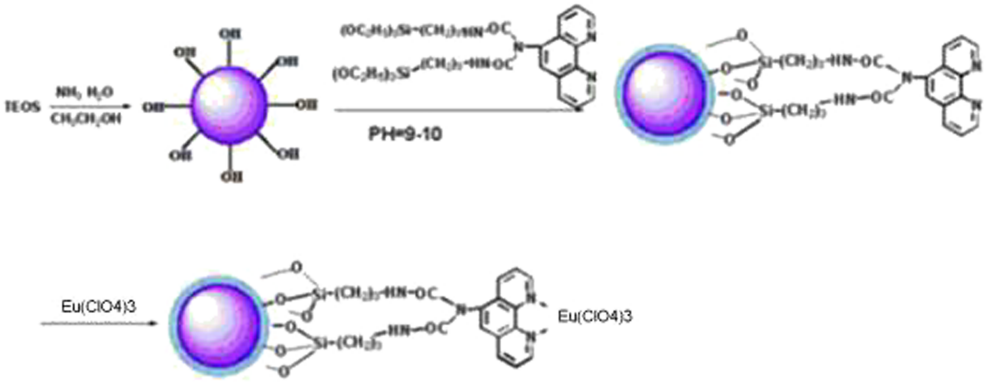

SCHEME 2 Self-assembly of SiO_2@Eu(phen–Si)$_3$(ClO_4)

shifted to 1699 cm^{-1} in nanometre luminescent composites that formed the core–shell structure (Figure S1d). ν-CONH– group stretching appeared at 1649 cm^{-1} and 1597 cm^{-1}. In nanometre luminescent composites with the core–shell structure, the ν-CONH– group expressed a lower wave number at 1598 cm^{-1} and 1504 cm^{-1}. The current results indicated that the Eu–phen–Si complex was composed of a shell layer of nanometre luminescent composite formed from a SiO_2 core and shell.

3.5 | Fluorescence spectra of the SiO_2@Eu(phen–Si) core–shell structure nanometre luminescent composites

In this study, excitation and emission spectra of the solid state material were tested at room temperature. Some excellent luminescence attributes were demonstrated by the nanometre luminescent composites that formed the core–shell structure (see spectra data in Figures 7–10 and Table 2).

The excitation spectra of the four types of composites structured by a SiO_2 core and shell ($SiO_{2(250)}$@Eu(phen–Si)$_{(10)}$, $SiO_{2(500)}$@Eu(phen–Si)$_{(50)}$, $SiO_{2(250)}$@Eu(phen–Si)$_{(5)}$ and $SiO_{2(500)}$@Eu(phen–Si)$_{(15)}$) demonstrated a peak related to the Eu ion at 612 nm. These excitation spectra were very similar, with many sharp peaks at 320–420 nm that belonged to excitation transitions of the Eu ions in the excitation spectra. The maximum peak appeared at 325 nm. The corresponding energy had a a wave number of *c*. 30,078 cm^{-1} that indicated that the strongest excitation peak was due to the $^7F_0 \rightarrow {}^5L_3$ transition of Eu^{3+}.[40,41] No energy transfer band for phen appeared in the excitation spectra. The observed excitation spectra could be due to the half-order of the 612 nm band or due to diffusion from the host SiO_2 matrix.

Five emission peaks in the fluorescence emission spectra (Figures 7(right) and 10(right)) were exhibited that contributed to the characteristic $^5D_0 \rightarrow {}^7F_J$ (J = 0, 1, 2, 3, 4) convection of Eu(III), corresponding emission peaks were at 579, 592, 612, 650 and 700 nm. The $^5D_0 \rightarrow {}^7F_2$ transition of Eu(III) at 612 nm was the strongest signal. The fluorescence emission intensity of these four nanometre luminescent composites formed by core–shell structure was very different under the same test conditions. $SiO_{2(250)}$@Eu(phen–Si)$_{(10)}$ has the largest fluorescence emission intensity, the strongest fluorescence emission peak intensity was 29,609 a.u. (Figure 7(left)). The second fluorescence emission intensity was $SiO_{2(500)}$@Eu(phen–Si)$_{(50)}$ with a strongest fluorescence emission peak intensity of 19,762 a.u. (Figure 8 (right)). The third fluorescence emission intensity was $SiO_{2(250)}$@Eu(phen–Si)$_{(5)}$ with the strongest peak intensity at 10,225 a.u. (Figure 9(right)). The final fluorescence emission intensity was $SiO_{2(500)}$@Eu(phen–Si)$_{(15)}$ with the strongest peak intensity

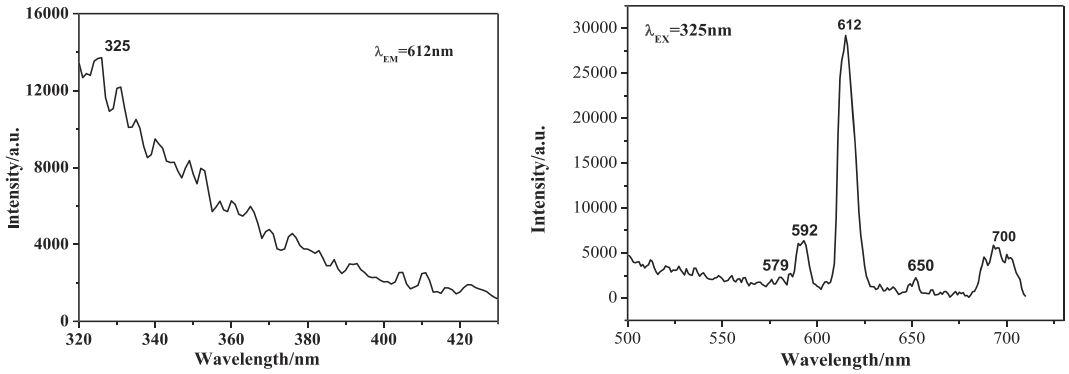

FIGURE 7 Fluorescence excitation spectrum (left) and fluorescence emission spectrum (right) of $SiO_{2(250)}$@Eu(phen–Si)$_{(10)}$

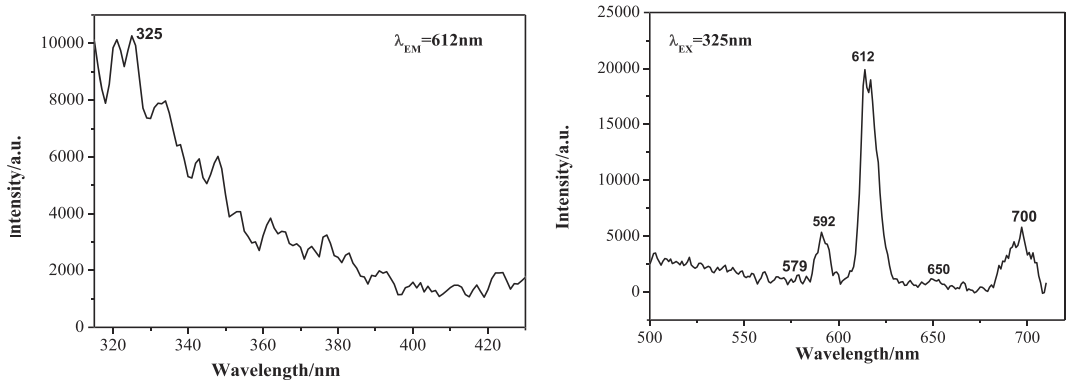

FIGURE 8 Fluorescence excitation spectrum (left) and fluorescence emission spectrum (right) of $SiO_{2(500)}$@Eu(phen–Si)$_{(50)}$

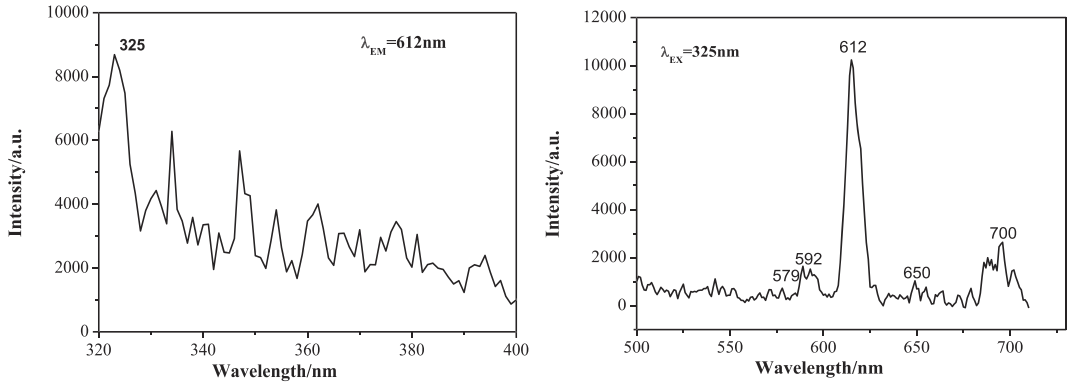

FIGURE 9 Fluorescence excitation spectrum (left) and fluorescence emission spectrum (right) of $SiO_{2(250)}$@Eu(phen–Si)$_{(5)}$

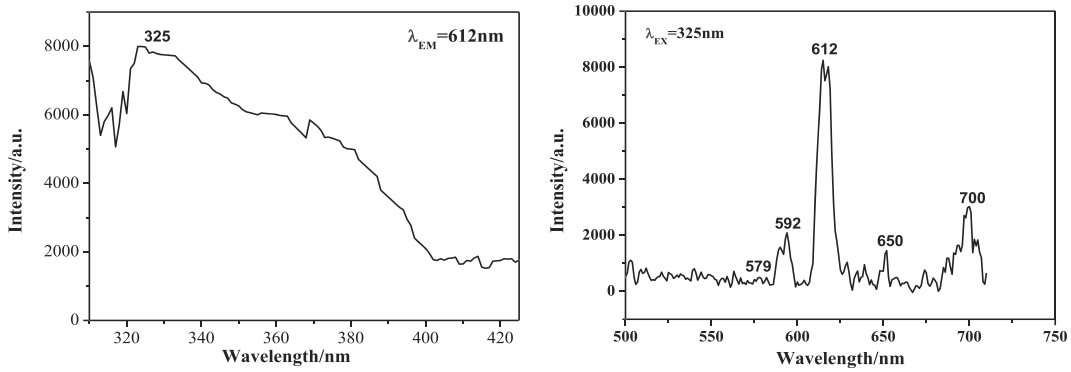

FIGURE 10 Fluorescence excitation spectrum (left) and fluorescence emission spectrum (right) of $SiO_{2(500)}$@Eu(phen–Si)$_{(15)}$

at 6543 a.u. (Figure 10(right)). These results showed that luminescence of the nanometre composites was affected by the structure of the core–shell. Kernel size and shell thickness will affect luminescence properties. By comparing Figure 7(left) and Figure 8(right), it can be seen that the fluorescence emission intensity of $SiO_{2(250)}$@Eu(phen–Si)$_{(10)}$ was 1.50-fold higher than that of $SiO_{2(500)}$@Eu(phen–Si)$_{(50)}$, indicating that luminescence properties improved when the kernel size of the core–shell structure nanometre luminescent composites was smaller. Comparing Figure 7(right) and Figure 9(right) or Figure 8(right) and Figure 10(right), it can be seen that the fluorescence emission intensity of the $SiO_{2(250)}$@Eu(phen–Si)$_{(10)}$ was 2.63-fold as great than that of $SiO_{2(250)}$@Eu(phen–Si)$_{(5)}$ or the fluorescence emission intensity of the $SiO_{2(500)}$@Eu(phen–Si)$_{(50)}$ was 3.02-fold greater than that of $SiO_{2(500)}$@Eu(phen–Si)$_{(15)}$. These findings indicated that increasing the cladding layer thickness improved the luminescence properties.

TABLE 2 Fluorescence emission spectra data of the core–shell structure luminescent composites

Core–shell composites	Slit width (nm)	λ_{ex} (nm)	λ_{em} (nm)	I (a.u.)	Energy transition
$SiO_{2(250)}$@Eu (phen–Si)$_{(10)}$	1.0	325	579	2061	$^5D_0 \rightarrow {}^7F_0$
			592	6289	$^5D_0 \rightarrow {}^7F_1$
			612	29609	$^5D_0 \rightarrow {}^7F_2$
			650	2278	$^5D_0 \rightarrow {}^7F_3$
			700	5620	$^5D_0 \rightarrow {}^7F_4$
$SiO_{2(500)}$@Eu (phen–Si)$_{(50)}$	1.0	325	579	1516	$^5D_0 \rightarrow {}^7F_0$
			592	5363	$^5D_0 \rightarrow {}^7F_1$
			612	19762	$^5D_0 \rightarrow {}^7F_2$
			650	1347	$^5D_0 \rightarrow {}^7F_3$
			700	5796	$^5D_0 \rightarrow {}^7F_4$
$SiO_{2(250)}$@Eu (phen–Si)$_{(5)}$	1.0	325	579	744	$^5D_0 \rightarrow {}^7F_0$
			592	1643	$^5D_0 \rightarrow {}^7F_1$
			612	10225	$^5D_0 \rightarrow {}^7F_2$
			650	1023	$^5D_0 \rightarrow {}^7F_3$
			700	2673	$^5D_0 \rightarrow {}^7F_4$
$SiO_{2(500)}$@Eu (phen–Si)$_{(15)}$	1.0	325	579	744	$^5D_0 \rightarrow {}^7F_0$
			592	1715	$^5D_0 \rightarrow {}^7F_1$
			612	6543	$^5D_0 \rightarrow {}^7F_2$
			650	602	$^5D_0 \rightarrow {}^7F_3$
			700	1315	$^5D_0 \rightarrow {}^7F_4$

3.6 | The fluorescence decay curve

Figures S2 and S3 show the fluorescence decrease, as well as the double exponential fit curve of $SiO_{2(500)}$@Eu(phen–Si)$_{(50)}$ and $SiO_{2(250)}$@Eu(phen–Si)$_{(10)}$.

Fluorescence lifetimes for the four composites were determined using the double exponential mode. Lifetime of the Eu(III) ion was calculated using eqns (1) and (2):

$$I_{(t)} = I_0 + A_1 \exp\left(-t_1/\tau_1\right) + A_2 \exp\left(-t_2/\tau_2\right) \quad (1)$$

$$< \tau > = \left(A_1\tau_1^2 + A_2\tau_2^2\right)/\left(A_1\tau_1 + A_2\tau_2\right) \quad (2)$$

where $I_{(t)}$ was the fluorescence intensity varying with time t, and τ_1 and τ_2 were lifetime. Lifetimes of the four nanometre luminescent complexes ($SiO_{2(250)}$@Eu(phen–Si)$_{(10)}$, $SiO_{2(500)}$@Eu(phen–Si)$_{(50)}$, $SiO_{2(250)}$@Eu(phen–Si)$_{(5)}$ and $SiO_{2(500)}$@Eu(phen–Si)$_{(15)}$) were 778.68 μs, 734.97 μs, 734.90 μs and 643.78 μs, respectively.

3.7 | Fluorescence quantum yield studies

Depending on the determination of fluorescence emission intensity and lifetime, the intrinsic luminescence quantum yields of the $^5D_0$ emission in the four core–shell nanometre luminescent composites were able to be determined. Quantum yield η, indicated distinctly the competition between the radiative processes and the nonradiative processes. Eqn (2) confirmed the η values of the result here:[42]

$$\eta = \frac{A_r}{A_r + A_{nr}} \quad (2)$$

where A_r and A_{nr} are radiative and nonradiative transition rates, respectively. The denominator in eqn (1) was determined from the lifetime of the emitting level ($1/\tau = A_r + A_{nr}$, where τ is fluorescence lifetime). For europium luminescence the value of A_r was calculated from eqn (3):

$$Ar = \sum A_{0J} = A_{00} + A_{01} + A_{02} + A_{03} + A_{04} \quad (3)$$

where, J is the final $^7F_{0\text{-}4}$. A_{0J} values could be calculated using eqn (4):

$$A_{0J} = A_{01}(I_{0J}/I_{01})(\nu_{01}/\nu_{0J}) \quad (4)$$

where, $\nu_{0J} = 1/\lambda_J$, and λ is wavelength. A_{01} is the Einstein coefficient of spontaneous emission between the $^5D_0$ and the $^7F_1$ Stark levels. The $^5D_0 \rightarrow {}^7F_1$ transition was not based on the local ligand field as shown by the Eu(III) ion and, therefore, may be used as a reference for the whole spectrum *in vacuo*, A_{01} = 14.65 s^{-1}. From the above equations, fluorescent quantum yields of the four core–shell

TABLE 3 Fluorescence quantum yield of core–shell structure luminescent composites

	$SiO_{2(250)}$@Eu (phen–Si)$_{(5)}$	$SiO_{2(250)}$@Eu (phen–Si)$_{(10)}$	$SiO_{2(500)}$@Eu (phen–Si)$_{(15)}$	$SiO_{2(500)}$@Eu (phen–Si)$_{(65)}$
ν_{00} (m^{-1})	17 271	17 271	17 271	17 271
ν_{01} (m^{-1})	16 863	16 863	16 863	16 863
ν_{02} (m^{-1})	16 340	16 340	16 340	16 340
ν_{03} (m^{-1})	15 385	15 385	15 385	15 385
ν_{04} (m^{-1})	14 286	14 286	14 286	14 286
I_{01} (a.u.)	1643	6289	1715	5363
I_{02}(a.u.)	10 225	29 609	6543	19762
I_{02}/I_{01}	6.22	4.71	3.82	3.68
τ (ms)	0.416	0.680	0.609	0.735
$1/\tau$	2403	1471	1643	1361
Ar	501.91	365.87	312.22	317.81
η%	20.89	24.87	19.00	23.35

composites ($SiO_{2(250)}$@Eu(phen–Si)$_{(10)}$, $SiO_{2(500)}$@Eu(phen–Si)$_{(50)}$, $SiO_{2(250)}$@Eu(phen–Si)$_{(5)}$ and $SiO_{2(500)}$@Eu(phen–Si)$_{(15)}$) were 24.87%, 23.35%, 20.89% and 19.00% respectively (Table 3). The result shows that these four core–shell composites gave higher quantum yield values.

4 | CONCLUSION

Four core–shell structure nanometre luminescent composites with different kernel sizes and different shell layer thicknesses ($SiO_{2(500)}$@Eu(phen–Si)$_{(50)}$, $SiO_{2(500)}$@Eu(phen–Si)$_{(15)}$, $SiO_{2(250)}$@Eu(phen–Si)$_{(5)}$ and $SiO_{2(250)}$@Eu(phen–Si)$_{(10)}$) were synthesized by changing synthesis conditions. These four composites were investigated using SEM, TEM, and IR spectra. Based on SEM photographs, regular microstructures, smooth surfaces, and moderate dispersity were found for the monodisperse spherical SiO_2. Based on TEM photographs, the Eu–phen–Si complex self-assembled on the monodispersed SiO_2 spheres, referred to as SiO_2@Eu(phen–Si) to synthesize the SiO_2 core and shell. Fluorescent spectra illustrated that the four nanometre luminescent composites with the core–shell structure had excellent luminescence attributes. The nanometre luminescent composites with a 250 nm kernel size exhibited stronger fluorescent than composites with a 500 nm kernel size. Fluorescence properties were affected by the thickness of the shell, such that when the shell thickness was thicker, the fluorescence intensity increased.

Quantum yields and fluorescence lifetimes of the four types of composites were calculated from fluorescence emission intensity data. Performance of the material in the SiO_2 core and shell, and the rare earth organic complex applied as the coating layer, was at the nanometre level. Use of lesser amounts of rare earth organic complexes decreased the cost.

The nanometre composites formed by the core–shell structure had excellent luminescence features for use as luminescent materials. This study provides available new areas for future research into new-style luminescent materials including information on europium luminescent materials and assistance on development and improvement in the application of Eu(III) rare earth elements.

ACKNOWLEDGEMENTS

This work was supported financially from Major Projects of the Natural Science Foundations of the Inner Mongolia Science Foundation (2015ZD01) and the Natural Science Foundations of the Inner Mongolia Science Foundation (2015MS0502).

ORCID

Wen-Xian Li https://orcid.org/0000-0002-0938-6910

REFERENCES

[1] Y. L. Liu, G. Cheng, Z. G. Wang, J. L. Zhang, D. H. Sun, G. Y. Hong, J. Z. Ni, *Mater. Lett. J.* **2013**, *97*, 187.

[2] L. N. Liu, B. Li, R. F. Qin, *Nanotechnology* **2010**, *21*, 285701.

[3] A. P. Duarte, M. Gressier, M. J. Menu, J. Dexpert-Ghys, J. M. A. Caiut, S. J. L. Ribeiro, *J. Phys. Chem. C* **2012**, *116*, 505.

[4] X. Y. Huang, *J. Alloy, Compd* **2015**, *628*, 240.

[5] S. H. Chung, D. W. Lee, M. S. Kim, K. Y. Lee, *J. Colloid Interface Sci.* **2011**, *355*, 70.

[6] H. Wang, J. Yang, C. M. Zhang, J. Lin, *J. Solid State Chem.* **2009**, *182*, 2716.

[7] X. Li, O. Niitsoo, A. Couzis, *J. Colloid Interface Sci.* **2016**, *465*, 333.

[8] J. Zeng, Y. Cao, C. H. Lu, X. D. Wang, Q. Wang, C. Y. Wen, J. B. Qu, C. Yuan, Z. F. Yan, X. Chen, *Anal. Chim. Acta* **2015**, *891*, 269.

[9] H. Zhang, D. Lin, G. Xu, J. Zheng, *Int. J. Hydrogen Energy* **2015**, *40*, 1742.

[10] A. A. Ansari, T. N. Hasan, N. A. Syed, J. P. Labis, A. K. Parchur, *Nanomedicine* **2013**, *9*, 1328.

[11] A. A. Ansari, J. P. Labis, *J. Mater. Chem.* **2012**, *22*, 16649.

[12] A. A. Ansari, L. Joselito, A. S. Aldwayyan, H. Mahmoud, *Nanoscale Res. Lett.* **2013**, *8*, 163.

[13] B. Koen, P. Lenaerts, K. Driesen, C. Gorller-Walrand, *J. Mater. Chem.* **2004**, *14*, 191.

[14] V. G. Pol, D. N. Srivastava, O. Palchik, V. Palchik, M. A. Slifkin, A. M. Weiss, A. Gedanken, *Langmuir* **2002**, *18*, 11312.

[15] K. Zhang, X. H. Zhang, H. T. Chen, X. Chen, L. L. Zheng, J. H. Zhang, B. Yang, *Langmuir* **2004**, *20*, 11312.

[16] M. Yu, H. Wang, C. K. Lin, G. Z. Li, J. Lin, *Nanotechnol.* **2006**, *17*, 3245.

[17] X. G. Liu, G. Y. Hong, *J. Solid State Chem.* **2005**, *178*, 1647.

[18] T. K. Tseng, J. H. Choi, M. Davidson, P. H. Holloway, *J. Mater. Chem.* **2010**, *20*, 6111.

[19] F. Zeb, A. R. Qureshi, K. Nadeem, M. Mumtaz, H. Krenn, *J. Non-Cryst. Solids* **2016**, *435*, 69.

[20] S. H. Zhang, L. Wen, J. P. Yang, Q. Sun, Z. Li, D. Zhao, S. X. Dou, *Part. Part. Syst. Charact.* **2016**, *33*, 261.

[21] E. W. Barrera, C. M. Pujol, C. Cascales, J. J. Carvajal, X. Mateos, R. Solé, J. Massons, M. Aguiló, F. Díaz, *Opt. Mater.* **2011**, *34*, 355.

[22] G. X. Liu, G. Y. Hong, D. X. Sun, *J. Colloid Interface Sci.* **2012**, *278*, 133.

[23] Y. J. Liang, O. Y. Jun, H. Y. Wang, W. L. Wang, P. F. Chui, K. N. Sun, *Appl. Surf. Sci.* **2012**, *258*, 3689.

[24] X. X. Ju, X. M. Li, Y. L. Yang, W. L. Li, C. Y. Tao, W. L. Feng, *J. Solid State Chem.* **2012**, *87*, 109.

[25] S. Cousinie, M. Gressier, C. Reber, J. Dexpert-Ghys, M. J. Menu, *Langmuir* **2008**, *24*, 6208.

[26] D. J. Zhang, D. H. Tang, X. M. Wang, M. Xue, Z. A. Qiao, Y. T. Li, Y. L. Liu, Q. S. Huo, *Dalton. Trans.* **2011**, *40*, 9313.

[27] A. C. Franville, R. Mahiou, D. Zambon, D. Zambon, J. C. Cousseins, *Solid State Sci.* **2011**, *3*, 211.

[28] H. R. Li, J. Lin, H. J. Zhang, L. S. Fu, Q. G. Meng, S. B. Wang, *Chem. Mater.* **2002**, *14*, 3651.

[29] Q. M. Wang, B. Yan, *Inorg. Chem. Commun.* **2004**, *7*, 747.

[30] Y. Li, B. Yan, *J. Solid State Chem.* **2008**, *181*, 1032.

[31] Z. Y. Yang, B. Yan, *Inorg. Chem. Commun.* **2014**, *47*, 96.

[32] B. Yan, C. Wang, *Inorg. Chem. Commun.* **2011**, *14*, 1494.

[33] X. M. Guo, H. D. Guo, L. S. Fu, H. J. Zhang, R. P. Deng, L. N. Sun, J. Feng, S. Dang, *Mesopor. Mat.* **2009**, *119*, 252.

[34] A. A. Ansari, A. K. Parchur, M. Alam, *A. Azzeer Spectrochimica Acta Part a* **2014**, *131*, 30.

[35] A. A. Ansari, A. K. Parchur, M. Alam, A. Azzeer, *Mater. Chem. Phys.* **2014**, *147*, 715.

[36] A. A. Ansari, M. Alam, J. P. Labis, S. A. Alrokayan, G. Shafi, *J. Mater. Chem.* **2011**, *21*, 19310.

[37] A. A. Ansari, A. K. Parchur, M. Alam, J. Labis, A. Azzeer, *J. Fluoresc.* **2014**, *24*, 1253.

[38] Q. M. Wang, B. Yan, *J. Mater. Chem.* **2004**, *14*, 2450.

[39] G. L. Davies, A. Barry, G. K. Yurii, *Chem. Physic. Lett.* **2009**, *468*, 239.

[40] C. Lin, D. Kong, X. Liu, H. Wang, M. Yu. Etal. **2007**, 46, 2674–2681.

[41] H. Ma. Inner Mongolia Normal University Graduate degree, **2017**(6): 39.

[42] A. Balamurugan, M. L. P. Reddy, M. Jayakanna, *J. Phys. Chem.* **2009**, *113*, 14128.

SUPPORTING INFORMATION

Additional supporting information may be found online in the Supporting Information section at the end of the article.

How to cite this article: Li W-X, Zheng Y-S, Zhang H-B, et al. Synthesis and characterization of luminescent SiO_2@Eu(phen–Si) core–shell nanospheres. *Luminescence*. 2019;1–10. https://doi.org/10.1002/bio.3721